12 Superconductivity and Magnetism

M. Bendele, S. Bosma, Z. Guguchia, L. Howald (since May 2011), H. Keller, A. Maisuradze, S. Siegrist, E. Stilp, S. Weyeneth

Visiting scientists: D. Di Castro, M. V. Eremin, B. I. Kochelaev, R. Puzniak, A. Shengelaya

Emeritus members: K. A. Müller (Honorarprofessor), T. Schneider (Titularprofessor), M. Mali, J. Roos

in collaboration with:
ETH Zürich (J. Karpinski, N. D. Zhigadlo), Paul Scherrer Institute (K. Conder, R. Khasanov, E. Morenzoni), Polish Academy of Sciences (R. Puzniak), Tbilisi State University (A. Shengelaya), MPI Stuttgart (J. Köhler, A. Bussmann-Holder), Kazan State University (M. V. Eremin, B. I. Kochelaev), EPFL Lausanne (H. Berger), IFW Dresden (P. Pahlke, B. Holzapfel), Universitá di Roma Tor Vergata (D. Di Castro), BAdW Garching, (A. Erb), University of Geneva (Ø. Fischer).

We report on research projects in the field of high-temperature superconductors (HTS's) and materials with novel electronic properties. Our studies involve various complementary techniques, such as muon-spin rotation (μSR), electron paramagnetic resonance (EPR), nuclear magnetic resonance (NMR), nuclear quadrupole resonance (NQR), and standard magnetometry techniques. Recent investigations on various interesting iron-based superconductors as well as first results obtained for magneto-electric Cu_2OSeO_3 are presented.

12.1 Pressure Effects in Iron-Chalcogenides

With the discovery of superconductivity in $LaFeAsO_{1-x}F_y$ [1], a new family of iron-based superconductors was found. Its simplest member is $FeSe_{1-x}$, consisting of a stack of FeSe layers. The superconducting properties of $FeSe_{1-x}$ [2] and $Fe_{1+y}Se_xTe_{1-x}$ [3] point to multigap superconductivity. We investigated the phase diagrams of $FeSe_{1-x}$ as a function of hydrostatic pressure [4] and of $Fe_ySe_{1-x}Te_x$ as a function of Te substitution [5] and amount of interstitial Fe [6] by means of muon-spin rotation (μSR), AC and DC magnetometry, and neutron diffraction. $FeSe_{1-x}$ is known to exhibit a large pressure effect on the superconducting transition temperature T_c. In addition, the pressure dependence $T_c(p)$ is non-uniform [4].

Unexpectedly, besides superconductivity coexisting magnetic order appears with pressure p, which is characterized by a magnetic transition temperature T_N much higher than T_c. As seen in Fig. 12.1

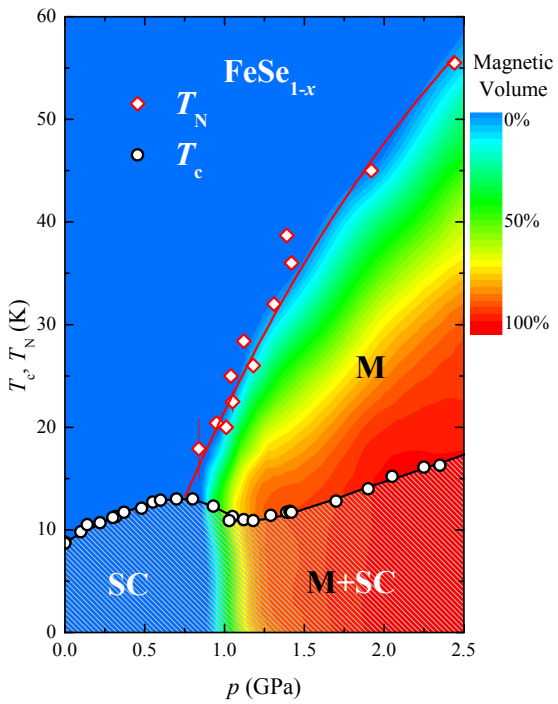

FIG. 12.1 – *Pressure dependence of T_c, T_N, and the superconducting and magnetic volume fractions in $FeSe_{1-x}$. The lines are guides to the eyes. SC and M denote the superconducting and magnetic states of the samples [7].*

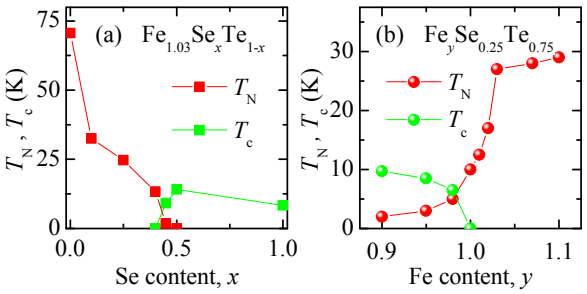

FIG. 12.2 – *Phase diagram of $Fe_ySe_xTe_{1-x}$ as a function of x (a) and y (b).*

magnetism and superconductivity are found to coexist microscopically for $T < T_c$ [4, 7]. Interestingly, substitution of Se by isovalent Te in the system $Fe_ySe_xTe_{1-x}$ has a similar effect. First, $T_c(x)$ increases, then superconductivity and magnetism coexist, and finally the material remains magnetic [5]. Recently, it turned out, that the superconducting and magnetic properties of $Fe_ySe_xTe_{1-x}$ not only depend on the Se-Te ratio x, but also strongly on the Fe content y [6, 8]. Upon fixing $x = 0.25$ and varying y one is able to tune the system from a coexistence region of magnetism and superconductivity to a state where the system is magnetic only (apart from traces of superconductivity, see Figs. 12.2 and 12.3). It was shown by us, that the magnetic correlation length decreases with decreasing amount of Fe. This rises the question whether Fe acts as an isolated moment that destroys superconductivity, or is an electron donor that suppresses superconductivity and induces weakly localized electronic states [6].

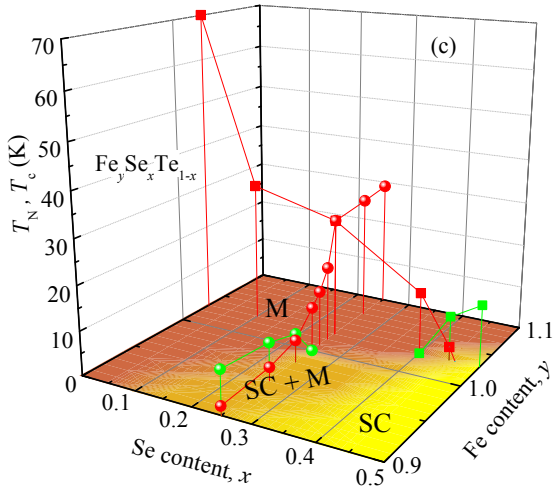

FIG. 12.3 – *Combination of panels (a) and (b) of Fig. 12.2 in a tentative three dimensional phase diagram. M and SC denote the magnetic and superconducting phases, respectively [6].*

[1] Y. Kamihara *et al.*, J. Am. Chem. Soc. **130**, 3296 (2008).

[2] R. Khasanov *et al.*, Phys. Rev. Lett. **104**, 087004 (2010).

[3] M. Bendele *et al.*, Phys. Rev. B **81**, 224520 (2010).

[4] M. Bendele *et al.*, Phys. Rev. Lett. **104**, 087003 (2010).

[5] R. Khasanov *et al.*, Phys. Rev. B **80**, 140511(R) (2009).

[6] M. Bendele *et al.*, Phys. Rev. B **82**, 212504 (2010).

[7] M. Bendele *et al.*, Phys. Rev. B **85**, 064517 (2012).

[8] R. Viennois *et al.*, J. Sol. St. Chem. **183**, 769 (2010).

12.2 Magnetic torque study of single-crystal $Rb_xFe_{2-y}Se_2$

A high $T_c \simeq 30$ K is also observed in the related iron-selenide family $A_xFe_{2-y}Se_2$ by intercalating alkali atoms between the FeSe layers [1]. Many reports [2, 3] indicate a coexistence of antiferromagnetism and superconductivity, with the antiferromagnetic domains corresponding to iron vacancy ordering. However, still no consensus for the values of the magnetic penetration depth λ and the magnetic penetration depth anisotropy γ_λ is found in literature.

We performed magnetic torque investigations on a single crystal of $Rb_xFe_{2-y}Se_2$ for various

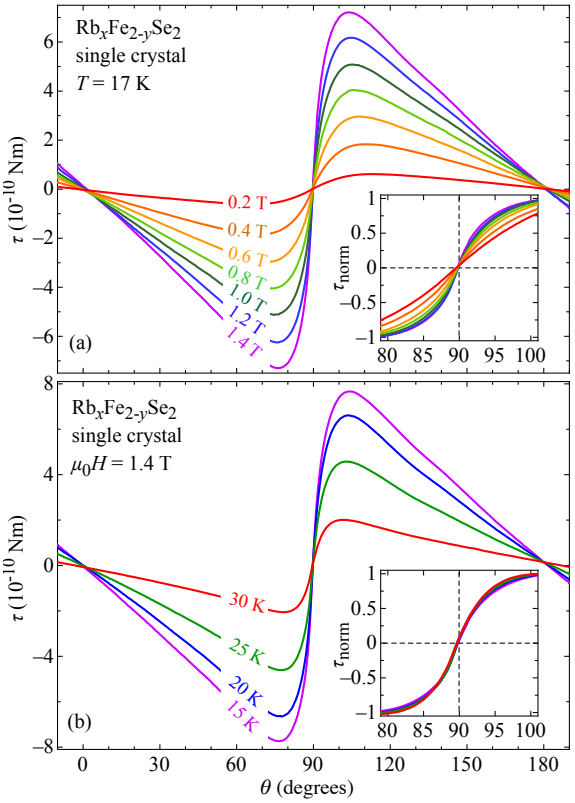

FIG. 12.4 – *Angular dependence of the superconducting component of the magnetic torque of $Rb_xFe_{2-y}Se_2$. (a) Magnetic torque at 17 K for various magnetic fields. (b) Magnetic torque at 1.4 T for various temperatures. The insets in both panels show the evolution of $\tau_{\rm norm} = \tau/\tau_{\rm max}$ close to the ab-plane [4].*

temperatures T and magnetic fields H applied with an angle θ with respect to the crystallographic c-axis of tetragonal $Rb_xFe_{2-y}Se_2$. A change of the slope of torque near the ab-plane ($\theta \sim 90°$) qualitatively reflects a change of γ_λ. Such a change of slope is evident from the torque data shown in Fig. 12.4, indicating that γ_λ depends on field, but not on temperature.

A detailed analysis of these data yields estimates for $\gamma_\lambda(T,H)$ and the effective magnetic penetration depth $\lambda_{\rm eff}(T,H)$. A summary of these results is shown in Fig. 12.5. The extrapolated value of $\lambda_{\rm eff}(0) \simeq 1.8$ μm is surprisingly large compared to other iron-based superconductors. However, measurements on the isotropic lower critical field H_{c1} are in good agreement with a rather large magnetic penetration depth in $Rb_xFe_{2-y}Se_2$. Intriguingly, microscopic techniques yield typical values of $\lambda \simeq 300$ nm [5]. It is possible that due to phase separation [3] in these materials, macroscopic techniques probing the effective magnetic penetration depth $\lambda_{\rm eff}$ yield substantially different values for λ than microscopic techniques.

A field dependent γ_λ may be associated with a complex band structure, since in the case of multiple superconducting gaps originating from different bands the superconducting screening currents, related to λ_{ab} and λ_c, may give rise to an unusual behavior of γ_λ. However, if a 2D-3D band scenario were the origin of the field dependence of γ_λ of $RbFe_{2-y}Se_2$, it should be temperature dependent as well [6] which is not the case according to Fig. 12.5d.

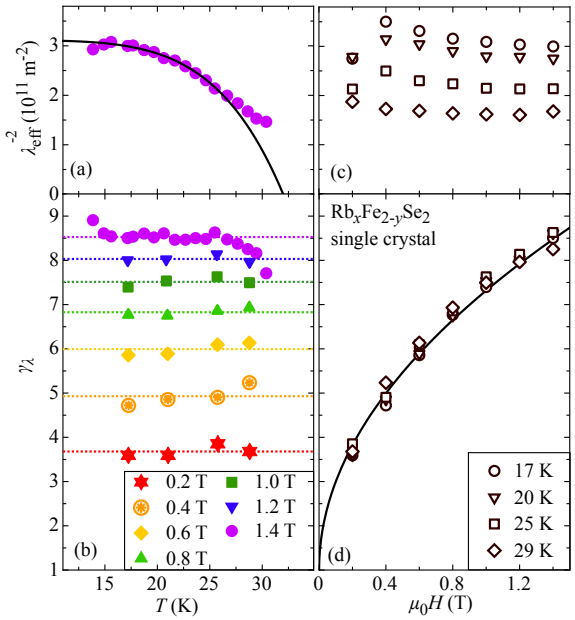

FIG. 12.5 – *Summary of all the results obtained from the torque data of $RbFe_{2-y}Se_2$. (a) Temperature dependence of $\lambda_{\rm eff}^{-2}$. The line is a power law fit to the data at 1.4 T. (b) Temperature dependence of γ_λ for various fields, showing that γ_λ is strongly increasing with H, but is almost independent of T. The dotted lines represent the average γ_λ for each field. (c) Field dependence of $\lambda_{\rm eff}^{-2}$ for various temperatures. (d) Field dependence of γ_λ for various T. The black line is a guide to the eye [4].*

A superconductor coexisting with an antiferromagnetic phase is expected to behave in a peculiar way. Varying the magnetic field can change the domain structure and the coupling between superconducting areas. This could result in variations of the averaged effective anisotropy. As was shown for various iron-based superconductors, the lattice parameters, in particular the pnictogen height in the iron-pnictides, are directly related to superconductivity [7]. Importantly, such scaling also works for the iron-selenide layer [7, 8]. It is possible that magnetostrictive effects, which are expected to increase with magnetic field, may influence the lattice parameters and consequently the anisotropy of the system.

[1] J. Guo *et al.*, Phys. Rev. B **82**, 180520 (2010).

[2] V. Ksenofontov *et al.*, Phys. Rev. B **84**, 180508 (2011).

[3] A. Ricci *et al.*, Phys. Rev. B **84**, 060511 (2011).

[4] S. Bosma *et al.*, Phys. Rev. B **85**, 064509 (2012).

[5] Z. Shermadini *et al.*, Phys. Rev. B **85**, 100501 (2012).

[6] M. Angst *et al.*, Phys. Rev. Lett. **88**, 167004 (2002).

[7] Y. Mizuguchi *et al.*, Supercond. Sci. Tech. **23**, 054013 (2010).

[8] A. Krzton-Maziopa *et al.*, J. Phys.: Condens. Matter **23**, 052203 (2011).

12.3 Anisotropic magnetic order in $EuFe_{2-x}Co_xAs_2$ single crystals

Among the iron-based pnictide HTS's, the family $EuFe_{2-x}Co_xAs_2$ is particularly interesting since Eu^{2+} is a rare-earth ion with a $4f^7$ electronic configuration and a total electron spin of $7/2$. This compound is built up by Fe_2As_2 layers, separated by layers of magnetic Eu^{2+} ions [1]. $EuFe_2As_2$ exhibits both a spin density wave (SDW) ordering of the Fe moments and an antiferromagnetic ordering of the localized Eu^{2+} moments below 190 K and 19 K, respectively [1, 2]. In contrast to related systems, where the substitution of Fe by Co leads to superconductivity [3], the compounds containing Eu^{2+} exhibit the onset of a superconducting transition, but seem to be hindered to reach zero resistivity at ambient pressure due to the AFM ordering of the Eu^{2+} spins [4, 5]. It is well established that the SDW state of the Fe moments is suppressed as a result of Co doping. However, at present there is no clear picture how the ordering of the Eu spins develops with increasing Co concentration. Thus, it is important to compare the magnetic properties of the Eu sublattice in $EuFe_{2-x}Co_xAs_2$ without and with Co doping in order to study the correlation between the ordering of the Eu^{2+} moments and the magnetism of the Fe sublattice. This is crucial to understand the interplay between magnetism of localized moments and superconductivity in $EuFe_{2-x}Co_xAs_2$.

A combination of magnetic susceptibility, magnetization, and magnetic torque experiments were performed on single crystals of $EuFe_{2-x}Co_xAs_2$ ($x = 0,\ 0.2$) [6]. The goal of this study is to investigate the macroscopic magnetic properties of the Eu sublattice. Magnetic susceptibility and magnetization investigations provide information on the magnetic structure of a single-crystal sample in magnetic fields applied along the principal axes. In addition, the evolution of the magnetic structure as a function of the tilting angle of the magnetic field and a crystallographic axis can be studied by magnetic torque. The results are summarized in Fig. 12.6 and 12.7. They are discussed in terms of the phase diagram of the Eu^{2+} magnetic sublattice of $EuFe_2As_2$ and $EuFe_{1.8}Co_{0.2}As_2$ for $H \perp c$ and $H \parallel c$. For the parent compound $EuFe_2As_2$ four different magnetic phases were identified (see Fig. 12.6a and b): a paramagnetic (PM), an antiferromagnetic (AFM), a canted antiferromagnetic (C-AFM), and a ferromagnetic (FM) phase. The present experiments suggest a C-AFM order of the Eu^{2+} spins in $EuFe_2As_2$ in the temperature range

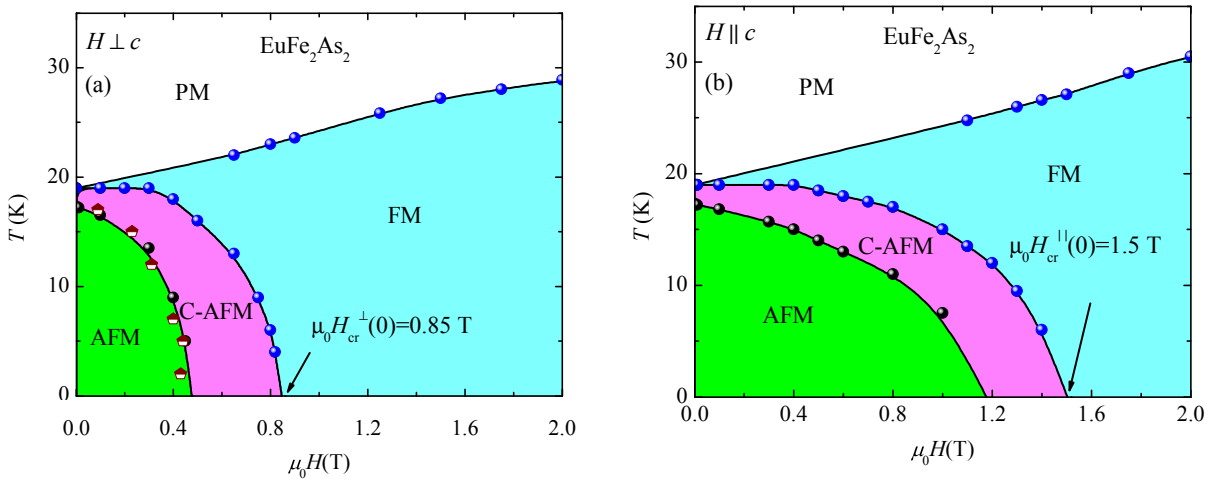

FIG. 12.6 – *Magnetic phase diagrams of single-crystal $EuFe_2As_2$ for $H \perp c$ and for $H \parallel c$. The various phases in the diagrams are denoted as: paramagnetic (PM), antiferromagnetic (AFM), canted antiferromagnetic (C-AFM), ferromagnetic (FM). The spheres and red&white symbols are from the susceptibility and field dependent magnetization measurements, respectively. Solid lines are guides to the eye [6].*

between 17 K and 19 K, while below 17 K an AFM structure is proposed. We also propose that at low temperatures the system can be well described by a uniaxial model with an easy plane and A-type AFM order. By applying a magnetic field within the AFM phase, a transition from AFM order via a canted configuration to a FM structure is observed. The corresponding magnetic phase diagrams for Co doped $EuFe_{1.8}Co_{0.2}As_2$ are shown in Fig. 12.7a and b. The magnetic ordering temperature of $\simeq$ 17 K is only about 2 K lower as compared to the parent compound. However, in the Co doped $EuFe_{1.8}Co_{0.2}As_2$, no signatures of a low-field and low-temperature AFM state of the Eu^{2+} moments was found. Only a C-AFM phase (with a FM component in the *ab*-plane) is present at low fields and low temperatures. The ordering temperature $T_{\mathrm{C-AFM}}$ decreases with increasing magnetic field, similar to the parent compound (see Fig. 12.7a and b). The critical magnetic field H_{cr} at which the Eu magnetic ordering is saturated was determined for different temperatures, and the extrapolated zero-temperature values were found to be strongly reduced with Co doping.

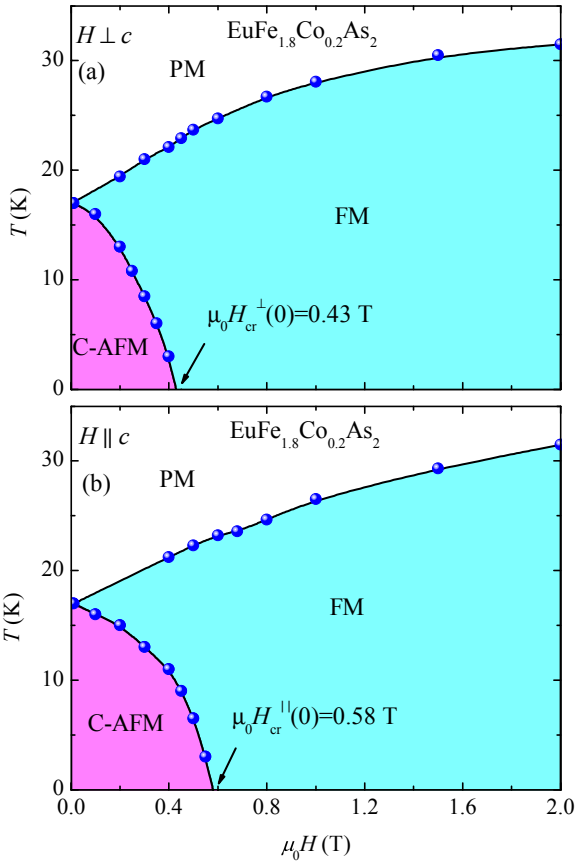

FIG. 12.7 – *Magnetic phase diagrams of single-crystal $EuFe_{1.8}Co_{0.2}As_2$ for $H \perp c$ and for $H \parallel c$. The meaning of the symbol is as in Fig. 12.6 [6].*

The present investigations reveal that the magnetic configuration of the Eu moments is strongly influenced by the magnetic moments of the Fe sublattice, where superconductivity takes place for a certain range of Co doping. This gives rise to a complex and sophisticated interplay of magnetic phases in $EuFe_{2-x}Co_xAs_2$. A detailed knowledge of the interplay between the Eu^{2+} moments and magnetism of the Fe sublattice is important to understand the role of magnetism of the localized Eu^{2+} moments for the occurrence of superconductivity in $EuFe_{2-x}Co_xAs_2$.

[1] H. Raffius *et al.*,
J. Phys. Chem. Solids **54**, 135 (1993).

[2] Y. Xiao *et al.*,
Phys. Rev. B **80**, 174424 (2009).

[3] A. S. Sefat *et al.*,
Phys. Rev. Lett. **101**, 117004 (2008).

[4] Y. He *et al.*,
J. Phys.: Condens. Matter **22**, 235701 (2010).

[5] Z. Guguchia *et al.*,
Phys. Rev. B **83**, 144516 (2011).

[6] Z. Guguchia *et al.*,
Phys. Rev. B **84**, 144506 (2011).

12.4 μSR study of the magnetoelectric coupling in Cu_2OSeO_3

Multiferroic and magnetoelectric materials are in the focus of research activities in recent years [1, 2]. The coupling between magnetic and electric parameters increases the degrees of freedom of the ordered ground state, making these materials good candidates for the study of new phenomena in highly correlated electronic systems. Strong magnetoelectric coupling is rather rare in solid state physics, since usual microscopic mechanisms for magnetic and electric polarization are mutually exclusive. Magnetism requires strong exchange interactions related to a strong hybridization of the transition ion electrons leading to conductivity. Conductivity, on the other hand, is inconsistent with the presence of an electric polarization in a sample [2]. The presence of large magnetic and electric polarizations is an important condition for strong magnetoelectric coupling, making ferro- or ferrimagnetic materials favorable candidates [1].

The ferrimagnetic magnetoelectric compound Cu_2OSeO_3 was recently discovered [3], and single crystals were successfully grown soon after [4]. The compound is piezoelectric and undergoes a ferrimagnetic transition below 60 K, exhibiting magnetoelectric coupling as revealed by magnetocapacitance studies on a polycrystalline sample [3]. An abrupt change of the dielectric constant below the ferrimagnetic transition was later confirmed by infrared studies [5, 6].

In this study we investigated the magnetic properties and the magnetoelectric coupling in Cu_2OSeO_3 by means of zero field and transverse field μSR in combination with alternating electric fields. A careful analysis of the electrostatic and magnetic field distributions in the lattice unit cell allowed us to identify possible muon stopping sites and corresponding local magnetic fields probed by the muon [7]. The obtained μSR spectra were found to be consistent with the ferrimagnetic structure below $T_C = 57.0(1)$ K [3]. In the low temperature limit an internal magnetic field $B_{int}(0) = 85.37(25)$ mT was detected at the interstitial muon stopping site. The temperature dependence of the internal magnetic is well described by the relation $B_{int} = B(0)(1 - (T/T_C)^2)^{\tilde{\beta}}$ with an effective exponent $\tilde{\beta} \simeq 0.39(1)$ which is close to the critical exponent $\beta \simeq 1/3$ for a three dimensional (3D) magnetic system (see Fig. 12.8). Just above T_C the muon relaxation rate follows the power law $\lambda(T) \propto (T/T_C - 1)^{-\tilde{\omega}}$ with $\tilde{\omega} = 1.06(9)$, which is characteristic for 3D ferromagnets. Measurements of $B_{int}(T)$ with and without an applied electrostatic field $E = 1.66 \times 10^5$ V/m suggest a electric field effect of magnitude $\Delta B_V = B_V(0\ \text{V}) - B_V(500\ \text{V}) = -0.4(4)$ mT [7].

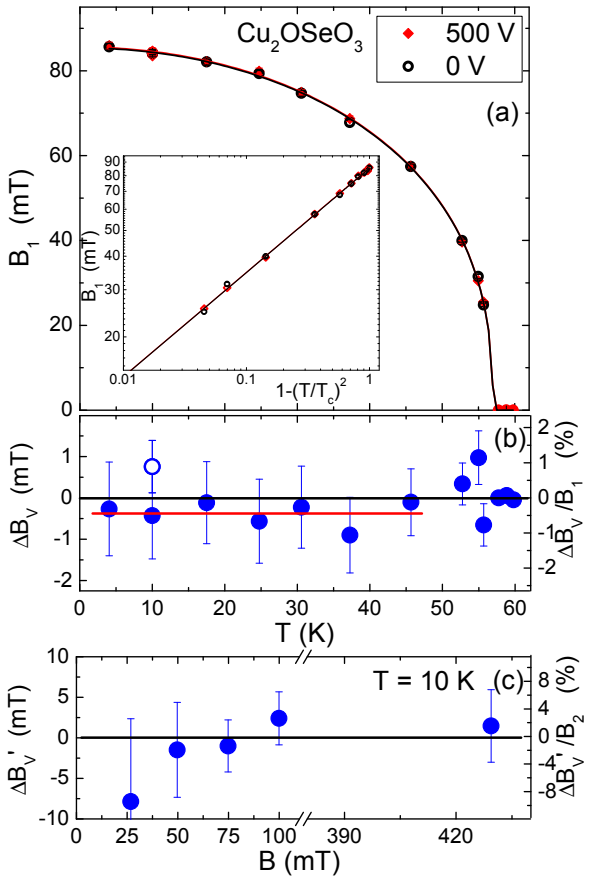

FIG. 12.8 – *(a) Temperature dependence of the mean internal B_1 field in single crystal Cu_2OSeO_3 for zero and applied electrostatic field E. The solid lines are power law fits to the data. The insert shows B_1 vs $(1-(T/T_C)^2)$ on a log-log scale. (b) Electric field shift $\Delta B_V = B_1(0\ V) - B_1(500\ V)$ as a function of temperature. The solid red line corresponds to the mean value of $\overline{\Delta B_V} \simeq -0.4(4)$ mT below 50 K. (c) Electric field shift $\Delta B'_V = \hat{B}_2(0\ V) - \hat{B}_2(800\ V)$ as a function of magnetic field measured by transverse field μSR at 10 K [7].*

[1] M. Fiebig, J. Phys. D: Appl. Phys. **38**, R123 (2005).

[2] N. A. Hill, J. Phys. Chem. B **104**, 6694 (2000).

[3] J.-W. G. Bos *et al.*, Phys. Rev. B **78**, 094416 (2008).

[4] M. Belesi *et al.*, Phys. Rev. B **82**, 094422 (2010).

[5] K. H. Miller *et al.*, Phys. Rev. B **82**, 144107 (2010).

[6] V. Gnezdilov *et al.*, Fiz. Nizk. Temp. **36**, 688 (2010).

[7] A. Maisuradze *et al.*, Phys. Rev. B **84**, 064433 (2011).